DRAFT VERSION FEBRUARY 5, 2008
Preprint typeset using LaTeX style emulateapj v. 10/10/03

WEIBEL FILAMENT DECAY AND THERMALIZATION IN COLLISIONLESS SHOCKS AND GAMMA-RAY BURST AFTERGLOWS

MILOŠ MILOSAVLJEVIĆ AND EHUD NAKAR
Theoretical Astrophysics, Mail Code 130-33, California Institute of Technology, 1200 East California Boulevard, Pasadena, CA 91125
Draft version February 5, 2008

ABSTRACT

Models for the synchrotron emission of gamma-ray burst afterglows suggest that the magnetic field is generated in the shock wave that forms as relativistic ejecta plow through the circum-burst medium. Transverse Weibel instability efficiently generates magnetic fields near equipartition with the post-shock energy density. The detailed saturated state of the instability, as seen in particle-in-cell simulations, consists of magnetically self-pinched current filaments. The filaments are parallel to the direction of propagation of the shock and are about a plasma skin depth in radius, forming a quasi–two-dimensional structure. We use a rudimentary analytical model to argue that the Weibel filaments are unstable to a kink-like mode, which destroys their quasi–two-dimensional structure. For wavelengths longer than than the skin depth, the instability grows at the rate equal to the speed of light divided by the wavelength. We calculate the transport of collisionless test particles in the filaments experiencing the instability and show that the particles diffuse in energy. This diffusion marks the beginning of thermalization in the shock transition layer, and causes initial magnetic field decay as particles escape from the filaments. We discuss the implications of these results for the structure of the shock and the polarization of the afterglow.

Subject headings: gamma-rays: bursts — MHD — instabilities — magnetic fields — plasmas — shock waves

1. INTRODUCTION

Gamma-ray bursts (GRB) afterglows have been ascribed to synchrotron emission from relativistic shocks in an electron-proton plasma. Detailed studies of GRB spectra and light curves have shown that the magnetic field strength in the shocked plasma (the downstream) is a fraction of $\epsilon_B \sim 10^{-2} - 10^{-3}$ of the internal energy, while the energy in the emitting electrons is a fraction of $\epsilon_e \sim 10^{-1}$ of the internal energy (Panaitescu & Kumar 2002; Yost et al. 2003). Recently, Eichler & Waxman (2005) have shown that if only a small fraction f of the electrons are accelerated into the high-energy nonthermal tail, the observations can be fitted with values of ϵ_B and ϵ_e that are smaller by a factor of f than the above estimates, as long as f is larger than the electron to proton mass ratio m_e/m_p. This still implies a magnetic field with $\epsilon_B \gtrsim 10^{-6}$. Furthermore, the measurement of linear polarization at the level of a few percent (Björnsson, Gudmundsson, & Jóhannesson 2004; Covino et al. 2004 and references therein) implies that the magnetic field in the synchrotron emitting region must deviate from isotropy.

Simple compressional hydrodynamic amplification of a pre-existing magnetic field of the unshocked plasma (the upstream) results in $\epsilon_B \sim 10^{-9}$ (Gruzinov 2001). Thus the requisite magnetic field must be generated in the shock itself or in the downstream. A leading candidate mechanism that produces a magnetic field near equipartition in the shock transition layer is the transverse Weibel instability (Weibel 1959; Fried 1959), as was suggested by Gruzinov & Waxman (1999) and Medvedev & Loeb (1999).[1] This instability and the magnetic field it produces are expected to play a crucial role in the thermalization of the upstream and in the shock dynamics.

Recently, a great progress toward understanding unmagnetized collisionless shocks has been made by means of two- and three-dimensional particle-in-cell (PIC) simulations (e.g., Lee & Lampe 1973; Gruzinov 2001; Silva et al. 2003; Frederiksen et al. 2004; Jaroschek et al. 2004; Medvedev et al. 2005; Kato 2005). Although the simulations do not resolve the *e–p* shock, they do show that within a layer ~ 100 proton skin depths wide, where the upstream and the downstream plasma interpenetrate, the transverse Weibel instability saturates.

The saturated state of the transverse Weibel instability consists of magnetically self-pinched current filaments (see, e.g., Fig. 1 in Frederiksen et al. 2004). The filaments are initially about a proton plasma skin depth in diameter and are parallel to the direction of shock propagation. As such they come with a magnetic field close to equipartition ($\epsilon_B \sim 0.1$) that lies in the plane perpendicular to the direction of shock propagation. However, the observed emission from GRB afterglows is expected to be produced at a distance of over $\sim 10^9$ plasma skin depths from the shock (e.g., Piran 2005 and references therein). Thus, even if the filamentary picture correctly describes the transition layer of GRB shocks, only the late evolution of these filaments is relevant for the observed emission.

Gruzinov (2001) pointed out that there is no obvious theoretical justification for the perseverance of the magnetic field. Since the field forms only on a small scale—the plasma skin depth—one would expect that it also decays over the small distance comparable to the skin depth. On the other hand, based on a quasi–two-dimensional picture of current filaments, Medvedev et al. (2005) suggest that the interaction between neighboring filaments may result in a magnetic field of an ever growing coherence length, whereby ϵ_B is saturated at a finite value many plasma skin depths in the downstream.

There are reasons to believe, however, that the quasi–two-dimensional picture is short-lived. For example, shock compression cannot be achieved in the region where the filaments make such an ordered structure (Milosavljević, Nakar, & Spitkovsky 2005). Lacking de-

[1] See Bret, Firpo, & Deutsch (2005) for a discussion of different modes of the Weibel instability.

tailed PIC simulations, however, the filament evolution, the isotropization of the upstream particles, and the production of shock jump conditions remain poorly understood. These processes, of course, are of immense importance for the microphysics of GRBs and collisionless shocks in general.

The two main processes that dictate the evolution the ordered outcome of the transverse Weibel instability are the magnetic self-confinement of each filament and the interactions between neighboring filaments. Here, we use simple analytical arguments to explore the first one, namely the stability of a single filament. In § 2, we present an MHD model of such current filament. In § 3, we show that the filament is unstable to a kink-like mode, and estimate the growth rate of the mode. This instability destroys the quasi–two-dimensional geometry of the filament and produces a significant magnetic field in the direction parallel to shock propagation. In § 4, we study the motion of collisionless test particles in the background of a current filament undergoing the instability. We show that charged particles confined within the filament diffuse in energy space. We suggest that this diffusion isotropisizes and thermalizes the upstream particles. In § 6, we discuss implications of these processes for the magnetic field decay and the physics of GRB afterglows.

2. EQUILIBRIUM WEIBEL FILAMENT

Consider a magnetostatic equilibrium composed of an infinite cylindrical current filament extending in the z direction. Let $r = 0$ be the center of the filament, where we use cylindrical coordinates (r,θ,z). Let the current flow in the $+z$ direction along the central axis. Further, assume that at some radius $r = R$, the current drops to zero. We refer to R as the radius of the filament. At $r > R$, there are currents flowing in other filaments in both directions ($\pm z$), so that the total current flowing through any given plane z = const vanishes. Since we are interested in the stability of a single filament, we ignore the effect on the filament of currents external to the filament.

Particles giving rise to the current must move coherently, e.g., if there is a pinching azimuthal magnetic field $B_\theta > 0$, positive charges move in the positive z-direction, and negative charges move in the negative z-direction. This is possible if the particles do not execute a full gyration in the magnetic field (Alfvén 1939); fractional gyrations give rise to directed current as explained in Spitzer (1965). This requirement implies that a filament's radial structure depends on its radius. A detailed discussion of this structure can be found in Davidson (1974) and Honda (2000); we here summarize the relevant aspects.

Consider first the regime in which the radius of the filament R is smaller than about the plasma skin depth, $R \lesssim \delta$. The skin depth equals $\delta \equiv c\gamma^{1/2}/\omega_{\rm p}$, where $\omega_{\rm p} \equiv (4\pi e^2 n/m)^{1/2}$ is the plasma frequency, γ is the kinetic Lorentz factor the particles, m is the mass of the particles, and n is their density (in $e^{\pm}$ shocks, m is the electron mass; in $e^{-}p$ shocks, it is the proton mass). This directly implies that the current flowing through the filament $I \sim \pi R^2 ne\beta_\parallel c$, where $\beta_\parallel c$ is the average axial velocity of particles in the filament, does not exceed the Alfvén critical current $I_{\rm A} = \gamma\beta_\parallel mc^3/e$. Since the magnetic field is related to the current via $B_\theta \sim I/Rc$, the condition $I \lesssim I_{\rm A}$ implies that the Larmor radius of the particle $r_{\rm L} = \gamma\beta mc^2/eB_\theta$ must exceed the radius of the filament $r_{\rm L} \gtrsim (\beta/\beta_\parallel)R > R$. As a result, when $R \lesssim \delta$, all particles magnetically confined to the filament move in directed fashion. Here $\beta_\parallel$ depends weakly on r and thus the current profile across the filament is approximately homogeneous.

However when $R > \delta$, if the current were uniform within $r \lesssim R$ and the average axial velocity of the current carrying charges were relativistic ($\beta_\parallel \sim 1$), the Larmor radius would be smaller than the radius of the filament, and directed motion of charges within the filament would be compromised. Directed current flow can still be maintained when $R > \delta$ if the current is confined within a thin annular cylindrical region of width ΔR not exceeding the Larmor radius. The current then gives rise to a thin magnetic "wall" against which a particle confined to the filament can be reflected. Then the Larmor radius within the current carrying layer can be written $r_{\rm L} = \delta^2/\Delta R$, and the condition $r_{\rm L} \geq \Delta R$ implies that the current carrying layer is thinner than the skin depth, $\Delta R \leq \delta$, as seen in PIC simulations. In this regime, the saturated phase of the transverse Weibel instability consists current-carrying domains separated by thin magnetic walls.

Analytic considerations (Milosavljević, Nakar, & Spitkovsky 2005) and numerical simulations indicate that once the transverse Weibel instability saturates in collisionless shocks, the filament size is comparable to the skin depth. Motivated by these results we focus here on the case in which $R \sim \delta$.

We assume that MHD equations apply and that the pressure tensor of the particles is isotropic. Both of these assumptions are oversimplifications. The pressure tensor near the axis of the filament is approximately isotropic when $r_{\rm L} \sim R \sim \delta$. The purpose of the MHD model is to elucidate the physical mechanisms and motivate specific collisionless PIC simulations of the saturated state of the Weibel instability. The simulations are the best way to test the theory over a range of parameter values.

The toroidal magnetic field $\mathbf{B} = B(r)\hat{\theta}$ is related to the axial current density $\mathbf{J} = J(r)\hat{\mathbf{z}}$ via

$$4\pi J = \frac{1}{r}\frac{d}{dr}(rB). \tag{1}$$

Within the MHD approximation, the fluid pressure $P(r)$ satisfies the equation of pressure equilibrium

$$\begin{aligned}\nabla P &= \mathbf{J}\times\mathbf{B}\\ &= -\frac{1}{8\pi r^2}\frac{d}{dr}(r^2B^2)\hat{\mathbf{r}}.\end{aligned} \tag{2}$$

To construct an magnetostatic equilibrium filament, one can choose the radial dependence of the magnetic field, and then evaluate the current density and the pressure using equations (1) and (2).

3. STABILITY

It immediately follows from equation (2) that the fluid pressure inside the filament is larger than outside, the magnetic pressure accounting for the difference. This pressure imbalance is the origin of the unstable behavior that we explore below. The filaments are unstable to the well-known sausage, kink, and related MHD modes (see., e.g., Hasegawa 1975 and references therein) which result in the distortion of the filament boundary. We here focus on a particular mode, the helical kink instability, but expect similar stability criteria, growth rates, and particle transport in other related modes.

Consider linear magnetostatic perturbations around the equilibrium described in § 2. According to the energy principle, elegantly proven in Kulsrud (2005), a perturbation given by the Lagrangian displacement $\vec{\xi}$ grows if the associated potential energy change is negative. The potential energy change

is given by (Bernstein et al. 1958)

$$W = \frac{1}{2}\int \left[\frac{Q^2}{4\pi} + \mathbf{J}\cdot(\xi\times\mathbf{Q}) + \gamma P(\nabla\cdot\vec{\xi})^2 + (\xi\cdot\nabla P)(\nabla\cdot\vec{\xi})\right] d\mathbf{x} \tag{3}$$

where $\mathbf{Q}\equiv\nabla\times(\vec{\xi}\times\mathbf{B})$ is the magnetic field perturbation, and the volume integral extends over all space in the radial direction and an averaging over z-direction is assumed.

Following Newcomb (1960), we consider a perturbation with displacement $\vec{\xi} = (\xi_r, \xi_\theta, \xi_z)$ of the form

$$\vec{\xi} = \mathrm{Re}[(\xi_r, i\xi_\theta, i\xi_z)e^{i(m\theta+kz)}] \tag{4}$$

where $\xi_r(r)$, $\xi_\theta(r)$, and $\xi_z(r)$ are real functions of radius. Newcomb shows that non-axisymmetric perturbations ($m\neq 0$) that minimize W are incompressible, $\nabla\cdot\vec{\xi} = 0$, and have form

$$\begin{aligned}
\xi_r &= \xi,\\
\xi_\theta &= \frac{i}{m}\left[\frac{d}{dr}(r\xi) - \frac{k^2r^4}{k^2r^2+m^2}\frac{d}{dr}\left(\frac{\xi}{r}\right)\right],\\
\xi_z &= \frac{ikr^3}{k^2r^2+m^2}\frac{d}{dr}\left(\frac{\xi}{r}\right).
\end{aligned} \tag{5}$$

Note that the function ξ, identical to the radial displacement ξ_r, has been left unspecified.

For perturbations of the form in equation (5), the potential energy perturbation in equation (3) can be expressed in terms of the radial displacement only,

$$W = \frac{\pi}{2}\int_0^\infty \left[f\left(\frac{d\xi}{dr}\right)^2 + g\xi^2\right] dr, \tag{6}$$

where

$$\begin{aligned}
f &\equiv \frac{rm^2B_\theta^2}{k^2r^2+m^2},\\
g &\equiv \frac{1}{r}\frac{m^2B_\theta^2}{k^2r^2+m^2} + \frac{1}{r}m^2B_\theta^2 - 2\frac{B_\theta}{r}\frac{d}{dr}(rB_\theta)\\
&\quad + m^2\frac{d}{dr}\left(\frac{B_\theta^2}{k^2r^2+m^2}\right),
\end{aligned} \tag{7}$$

as shown in equations (16-18) of Newcomb (1960) (note that in our case $B_z = 0$).

The perturbations with $m = 1$ are special in that they need not vanish at $r = 0$ and do not incur substantial cost in magnetic energy as the field lines are bent only minimally. Therefore one is allowed to assume that the radial displacement is independent of radius, $d\xi/dr = 0$, over the region with the non-vanishing magnetic field, which greatly simplifies the analysis. The true fastest growing mode may not have constant ξ, but one expects the constant ξ approximation to come close. For these perturbations the radial displacements are

$$\begin{aligned}
\xi_r &= \xi = \mathrm{const},\\
\xi_\theta &= i\left(1 + \frac{k^2r^2}{k^2r^2+1}\right)\xi,\\
\xi_z &= -\frac{ikr}{k^2r^2+1}\xi.
\end{aligned} \tag{8}$$

With this, the energy per unit length along the z-direction becomes

$$W = -\frac{\pi}{2}k^2\xi^2\int_0^\infty \frac{rB_\theta^2}{k^2r^2+1}dr. \tag{9}$$

Equation (9) tells us that all wave numbers $k > 0$ are unstable. In the long and the short wavelength limits, the energy can approximately be written as

$$W \approx \begin{cases} -\frac{1}{4}\pi\xi^2k^2R^2\bar{B}_\theta^2, & (kR\ll 1)\,,\\ -\frac{1}{2}\pi\xi^2\tilde{B}_\theta^2, & (kR\gg 1)\end{cases} \tag{10}$$

where $\bar{B}_\theta$ is the RMS magnetic field, and $\tilde{B}_\theta$ is the magnetic RMS field averaged per unit log-radius.

Equation (9) tells us that all $m = 1$ modes with finite wavelengths ($k > 0$) are unstable. An estimate of the linear growth rate is given by

$$\Gamma \sim \sqrt{-\frac{W}{K}}, \tag{11}$$

where

$$K \equiv \frac{1}{2}\int \rho(\xi_r^2 + \xi_\theta^2 + \xi_z^2) r d\theta dr. \tag{12}$$

The value of K for perturbations in equations (8) equals

$$K = \frac{\pi\bar{\rho}\xi^2}{4k^2}[5k^2R^2 - 3\ln(k^2R^2+1)] \tag{13}$$

where $\bar{\rho}$ is the average mass density. In the long and the short wavelength limit, therefore,

$$\Gamma \sim \begin{cases} k\bar{B}_\theta/\sqrt{2\bar{\rho}}, & (kR\ll 1)\,,\\ R^{-1}\tilde{B}_\theta/\sqrt{5\bar{\rho}/2}, & (kR\gg 1)\,.\end{cases} \tag{14}$$

Note that the growth rates are proportional to the "nonrelativistic" Alfvén velocity $\bar{v}_\mathrm{A}\equiv B_\theta/\sqrt{4\pi\bar{\rho}}$ multiplied by k and R^{-1}, respectively, in the long and the short wavelength limit. This is expected since the instability is driven by a pressure imbalance. The growth rate in the long wavelength limit can also be expressed as $\Gamma\sim(\pi/2)^{1/2}\beta_\parallel kR\omega_\mathrm{p}$, where as before ω_p is the plasma frequency.

Note that the magnetic field acquires a component parallel to the axis of the filament. The RMS strength of the parallel field is $\bar{B}_z = \bar{Q}_z \sim \frac{1}{2}k\xi B_\theta$ in the long wavelength limit.

The above analysis is valid only as long as the perturbation is nonrelativistic (i.e., $\xi < c/\Gamma$) and the wavelength of the perturbation is larger than the Larmor radius. Since we here consider the filaments with $r_\mathrm{L}\sim R\sim\delta$, the analysis is valid only for wavelengths with $2\pi/k \gtrsim r_\mathrm{L} \gtrsim \delta$. In such filaments the growth rate is $\Gamma\sim\beta_\parallel ck$.

4. TRANSPORT IN AN UNSTABLE FILAMENT

We next address the orbits of collisionless test particles in the electromagnetic field defined by the magnetostatic equilibrium (§ 2) and the linear unstable perturbation (§ 3). Consider a particle with unperturbed orbit confined to the region $r < R$, and assume that the motion is directed along the axis, $dz/dt > 0$. The momentum of the particle $\mathbf{p}$ is then a periodic function of z, as are its radial excursion and azimuth. The magnetostatic equilibrium is electrically neutral and the energy of the particle, $\mathcal{E} = \gamma mc^2$, where $\gamma\equiv(1+p^2/m^2c^2)^{1/2}$, subject to the magnetic field of the equilibrium only, is a constant of motion. The time variation of the magnetic field of the unstable perturbation induces an electric field given by Ohm's law

$$\mathbf{E} = -\frac{\mathbf{V}\times\mathbf{B}}{c}, \tag{15}$$

where $\mathbf{B}$ is the magnetic field of the equilibrium, and $\mathbf{V}\equiv d\vec{\xi}/dt$ is the bulk velocity associated with the perturbation.

In long wavelength perturbations, the displacement is mainly perpendicular to the z-axis and the electric field is thus mainly parallel to the axis.

In writing equation (15), we have assumed infinite conductivity, and have ignored terms of the form $\mathbf{J}\times\mathbf{B}$, $\partial\mathbf{J}/\partial t$, and ∇P. These terms can be neglected to the first order in $k\delta$ and $\Gamma/\omega_{\rm p}$, i.e., for wavelengths longer than the plasma skin depth.

Kinetic energy of a test particle with charge q incurs a change of

$$\Delta\mathcal{E} = q\int_{-\infty}^{t}\frac{\mathbf{p}\cdot\mathbf{E}}{\gamma m}dt'. \tag{16}$$

To the first order in the perturbation, the energy change equals

$$\begin{aligned}\Delta\mathcal{E} &= -q\Gamma\int_{-\infty}^{t}\beta\cdot(\vec{\xi}\times\mathbf{B})dt' \\ &= -q\Gamma\int_{-\infty}^{t}[\xi_z\beta_r\sin(kz+\theta) \\ &\qquad +\xi_r\beta_z\cos(kz+\theta)]e^{\Gamma t'}B_\theta dt', \end{aligned}\tag{17}$$

where $\beta\equiv\mathbf{p}/\gamma mc$ and as before Γ denotes the growth rate of the instability.

The energy change can be evaluated for the incompressible perturbations given in equations (8). The displacement of the fluid is an oscillatory function of the monotonic variable $z(t)$, as is the displacement of the particle. Resonances occur when $\beta_\parallel ck\sim\omega_\theta$, where $\beta_\parallel c$ is the average axial velocity of the particle, and ω_θ is its azimuthal angular frequency, which will differ from one particle to another. At a resonance, the particle experiences a coherent electric field over most of its orbit.

5. THERMALIZATION

To explore the effect of energy change derived in equation (17), we consider the simplest Maxwell-Vlasov equilibrium of a magnetically self-pinched current filament (Hammer & Rostoker 1970; Davidson 1974), in which all particles have the same total energy $\mathcal{E}=\gamma_0 mc^2$ and the same axial canonical momentum $\mathcal{P}_z=\beta_\parallel\gamma_0 mc$, both of which are constants of motion. Here, γ_0 is the Lorentz factor of the particles and $0<\beta_\parallel<(1-\gamma_0^{-2})^{1/2}$ is a constant. The canonical momentum equals $\mathcal{P}=\mathbf{p}-(e/c)\mathbf{A}$, where $\mathbf{A}$ is the vector potential.

Particle density n inside the filament associated with this equilibrium is uniform. The equilibrium has phase-space distribution function

$$f(\mathcal{E},\mathcal{P}_z)=\frac{n}{2\pi\gamma_0 m}\delta(\mathcal{E}-\gamma_0 mc^2)\delta(\mathcal{P}_z-\beta_\parallel\gamma_0 mc), \tag{18}$$

where $\delta(x)$ is the Dirac delta-function, not to be confused with the skin depth. The magnetic field and the vector potential inside the filament are given by

$$\begin{aligned}B_\theta &= -\frac{\beta_\parallel\gamma_0 mc^2}{e\delta}I_1\left(\frac{r}{\delta}\right), \\ A_z &= -\frac{\beta_\parallel\gamma_0 mc^2}{e}\left[1-I_0\left(\frac{r}{\delta}\right)\right], \end{aligned}\tag{19}$$

where as before δ is the plasma skin depth inside the filament, and $I_n(x)$ is the modified Bessel function of the first kind. The filament radius R is the solution of the equation

$$I_0^2\left(\frac{R}{\delta}\right)=\frac{\gamma_0^2-1}{\gamma_0^2\beta_\parallel^2}. \tag{20}$$

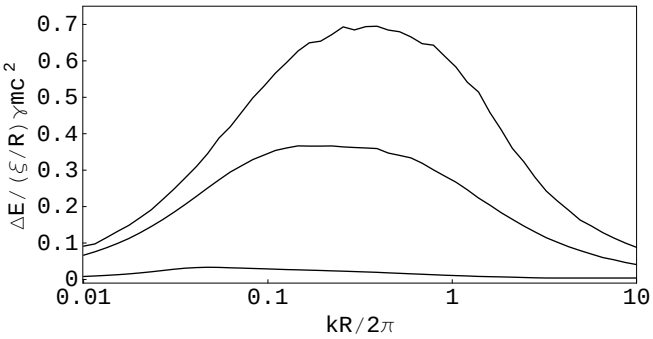

FIG. 1.— The RMS linear energy change $\Delta\mathcal{E}$ of a particle in units of $(\xi/R)\gamma mc^2$ as a function of the wave number k for the model described in § 5 with $\beta_\parallel=(0.05,0.5,0.95)$ from top to bottom and $\gamma_0=10$. Here, ξ is the final value of the displacement associated with the instability discussed in § 3. The energy change was calculated using Monte-Carlo integration.

Although extremely simple, this model correctly captures many of the characteristics of current filaments seen in PIC simulations, including the concentration of the current flow near the edge of the filament when $R\gtrsim\delta$.

Figure 1 shows the RMS linear energy change of particles drawn from the distribution of equation (18) with $\beta_\parallel=(0.05,0.5,0.95)$ as a function of the wave number k of the unstable perturbation. The magnetic field of the equilibrium filament is given by equations (19), and the filament is undergoing instability with displacement given in equations (8) and growth rate defined by equations (9), (11), and (12). For $\beta_\parallel\gtrsim 0.5$, the linear energy change is maximum for $kR\sim(0.1-0.4)\times 2\pi$. It should be kept in mind, however, that the pressure tensor in filaments with $\beta_\parallel\ll 0.5$ and those with $1-\beta_\parallel\ll 0.5$ is anisotropic, and thus the growth rates calculated in § 3 may not be accurate.

The instability affects in a similar way the pitch angle of the particles; the pitch angle can be defined as the angle subtended to the central axis at the instance of closest approach to the axis. We have focused on the energy because it is a simpler calculation.

As the orbits of particles inside a filament are perturbed by the instability, some of the particles that are initially confined to the filament escape. For example, consider a particle moving in the meridional plane ($\theta=$ const) that has radial velocity β_r when crossing the central axis. Assume that the particle is marginally confined to the filament, i.e., $\beta_r^2\sim R/r_{\rm L}$, where $r_{\rm L}\sim\gamma mc^2/e\bar{B}_\theta$ is the approximate Larmor radius. Evidently, an increase of the pitch angle $\phi=\sin^{-1}[\beta_r(1-\gamma^{-2})^{-1/2}]$ at a constant γ, or an increase of the energy $\mathcal{E}=\gamma mc^2$ at a constant pitch angle, both caused by the perturbed electromagnetic field of the instability discussed above, can liberate the particle from the filament.

A filament experiencing a growing kink instability continuously sheds particles in this fashion. The liberated particles have sufficient energy to visit neighboring filaments of either sign of the current, and can be thought of having joined a thermalized pool. The loss of particles implies decrease of the current flowing through the filament, which in turn implies the decay of the magnetic field. Only the particles that remain confined to the filaments contribute to the coherent toroidal magnetic field of the filament. Rapid field decay can be partially offset by an increase in the current per particle by electric fields induced during flux loss; robustness of the currents depends on the competition between the scattering and

the induction.

6. DISCUSSION

We have argued that the quasi–two-dimensional structure of the transition layer in collisionless shocks is disrupted by pressure-driven instabilities. We have also shown that the disruption is accompanied by a redistribution of particle energies, which can be interpreted as the onset of thermalization and magnetic field decay. Long term evolution of the magnetic field must therefore be addressed in the context of the three-dimensional turbulence that ensues after the Weibel filaments have been disrupted. The latter regime remains poorly understood.

An alternate interpretation of the early decay of the magnetic field refers to the hierarchical merging of current filaments due to Lorentz forces (Gruzinov 2001; Medvedev et al. 2005; Kato 2005). It can be asked whether the merging or the pressure-driven instabilities prevail. Since the maximum current that can flow through a filament is limited (see § 2), magnetic energy density must eventually decay under merging. However, PIC simulations of $e^{\pm}$ shocks (Spitkovsky & Arons 2005, private communication) show that the current inside a filament is tightly shielded by a reverse current flowing just outside the filament, i.e., opposite current filaments are tightly packed and most of the current flows near the edge. The shielding currents reduce the Lorentz attraction and slow the growth of the magnetic field correlation length via merging.

Meanwhile, the filaments are susceptible to the instabilities independently of the shielding. Therefore, we expect the dynamics of single filaments to be governed by the instabilities. In particular, the instabilities may drive merging between the filament fragments in three dimensions. The highest-resolution published simulations of cold shell collisions with two particle species by Frederiksen et al. (2004) show clear evidence for progressive bending and kinking of the "proton" ($m_p/m_e = 16$) filaments (see their Fig. 2).

Similar mechanism was recently studied by Zenitani & Hoshino (2005), who carried out two-dimensional PIC simulations of the relativistic drift-kink instability in an infinite $e^{\pm}$ current sheet confined between reversed magnetic fields. As the sheet bends in the direction perpendicular to the magnetic field, an alternating electric field is induced parallel to the sheet. The authors compare the growth rates measured in the simulations with predictions from two-fluid theory and find good agreement for $k\lambda \lesssim 0.7$, where k is the wave number and λ is the thickness of the current sheet. They also find that in the nonlinear stage of the instability, the electric field becomes coherent in the central region of the current sheet, which accelerates particles and efficiently dissipates the magnetic energy energy.

If external shocks in GRBs resemble the observed outcome of relativistic shell collisions in PIC simulations, the instability discussed here has implications for the interpretation of the observed weak linear polarization of the afterglow. The optical emission of GRB afterglows is linearly polarized at a level of a few percent, implying that the magnetic field in the emitting region is anisotropic. There are two different forms of magnetic field anisotropy that can produce this polarization. The first is a field parallel to the plane of the shock that is coherent on scales exceeding the plasma skin depth by many orders of magnitude (Gruzinov & Waxman 1999; Granot 2003). The second is a combination of a random magnetic field within the plane of the shock and a non-axisymmetric geometry of the emitting region (Gruzinov 1999; Sari 1999; Ghisellini & Lazzati 1999; Granot & Königl 2003; Nakar, Piran, & Waxman 2003; Rossi et al. 2004).

A coherent magnetic field within the plane of the shock is unlikely to be produced in the shock itself since there is no preferred direction within the plane of the shock. Such field could in principle result by amplification of a pre-existing, ambient coherent magnetic field. This possibility, however, is implausible because the field in the medium into which the GRB ejecta plow is expected to be far too weak. The second possibility is that the coherence length of the magnetic field generated the shock grows rapidly. Since at any given time the observer sees many causally disconnected regions (Gruzinov & Waxman 1999; Nakar & Oren 2004), the coherence length of the downstream magnetic field should grow at a rate close to the speed of light in order to produce a polarization at the level of a few percent. We do not know of a mechanism that would facilitate such growth, especially given that the Alfvén speed in the weakly magnetized relativistic downstream plasma is much smaller than the speed of light.

An anisotropic field, but random within the plane of the shock, appears to be a much more appealing possibility because the shock breaks the isotropy and could in principle result in a different mean field strength in the parallel and the perpendicular direction. In this case the level of polarization also depends on the degree to which the axisymmetry of the emitting region is broken. Assuming that the magnetic field lies entirely in the plane of the shock (i.e., $B_z = 0$), and that the geometry of the emitting region is as expected during the jet-break in the light curve, the level of polarization is at most $20\% - 30\%$ (Sari 1999; Rossi et al. 2004) and in some scenarios it can be as small as a few percent. If $B_z \approx B_{xy}$, the polarization level is significantly reduced. Therefore, the typical observed polarization of a few percent requires that either $B_z < B_{xy}/2$ or $B_z > 2B_{xy}$. Even this minor difference between B_z and B_{xy} presents a theoretical challenge in view of our results, which suggest that B_z arises quickly within the transition layer as the current filaments associated with the small-scale magnetic fields are effectively destroyed. We speculate that the magnetic field quickly becomes isotropic in the rest frame of the shocked plasma.

We are indebted to P. Goldreich and T. Piran for comments and advice, and J. Arons and A. Spitkovsky for many inspiring discussions and for sharing their numerical simulations with us ahead of publication. This work was supported at Caltech by a postdoctoral fellowship to M. M. and a senior research fellowship to E. N. from the Sherman Fairchild Foundation.

REFERENCES

Alfvén, H. 1939, Phys. Rev., 55, 425
Bernstein, I. B., Frieman, E. A., Kruskal, M. D., & Kulsrud, R. M. 1958, Proc. Roy. Soc., A244, 17
Björnsson, G., Gudmundsson, E. H., & Jóhannesson, G. 2004, ApJ, 615, L77
Bret, A., Firpo, M. C., & Deutsch, C. 2005, Phys. Rev. Lett., 94, 115002
Covino, S., Rossi, E., Lazzati, D., Malesini, D., & Ghisellini, G. 2004, preprint (astro-ph/0412129)
Davidson, R. C. 1974, Frontiers in Physics, 43 (Reading: W. A. Benjamin)
Eichler, D., & Waxman, E. 2005, ApJ, 627, 861

Frederiksen, J. T., Hededal, C. B., Haugbølle, T., Nordlund, Å. 2004, ApJ, 608, L13
Fried, B. D. 1959, Phys. Fluids, 2, 337
Ghisellini, G., & Lazzati, D. 1999, MNRAS, 309, L7
Granot, J. 2003, ApJ, 596, L17
Granot, J., & Königl, A. 2003, ApJ, 594, L83
Gruzinov, A. 1999, ApJ, 525, L29
Gruzinov, A. 2001, ApJ, 563, L15
Gruzinov, A., & Waxman, E. 1999, ApJ, 511, 852
Hammer, D. A., & Rostoker, N. 1970, Phys. Fluids, 13, 1831
Hasegawa, A. 1975, Plasma Instabilities and Nonlinear Effects (New York: Springer)
Honda, M. 2000, Phys. Plasmas, 7, 1606
Jaroschek, C. H., Lesch, H., & Treumann, R. A. 2004, ApJ, 616, 1065
Kato, T. N. 2005, preprint (physics/0501110)
Kulsrud, R. M. 2005, Plasma Physics for Astrophysics (Princeton: Princeton)
Lee, R., & Lampe, M. 1973, Phys. Rev. Lett., 31, 1390
Medvedev, M. V., & Loeb, A. 1999, ApJ, 526, 697
Medvedev, M. V., Fiore, M., Fonseca, R. A., Silva, L. O., & Mori, W. B. 2005, ApJ, 618, L75
Milosavljević, M., Nakar, E., & Spitkovsky, A. 2005, preprint (astro-ph/0507553)
Nakar, E., Piran, T., & Waxman, E. 2003, J. Cosmology Astropart. Phys., 10, 5
Nakar, E., & Oren, Y. 2004, ApJ, 602, L97
Newcomb, W. A. 1960, Ann. Phys., 10, 232
Panaitescu, A., & Kumar, P 2002, ApJ, 571, 779
Piran, T. 2005, preprint (astro-ph/0503060)
Rossi, E. M., Lazzati, D., Salmonson, J. D., & Ghisellini, G. 2004, MNRAS, 354, 86
Sari, R. 1999, ApJ, 524, L43
Silva, L. O., Fonseca, R. A., Tonge, J. W., Dawson, J. M., Mori, W. B., & Medvedev, M. V. 2003, ApJ, 596, L121
Spitzer, L. 1965, Physics of Fully Ionized Gases (Interscience: New York)
Weibel, E. S. 1959, Phys. Rev. Lett., 2, 83
Yost, S. A., Harrison, F. A., Sari, R., & Frail, D. A. 2003, ApJ, 597, 459
Zenitani, S., & Hoshino, M. 2005, ApJ, 618, L111